Publications of the Astronomical Society of the Pacific, 132:024201 (18pp), 2020 February https://doi.org/10.1088/1538-3873/ab6279


# Newly Discovered Period Changes in Two mCP Stars and Updates for Previously Published Stars

Diane M. Pyper[1] and Saul J. Adelman[2]
[1] Physics/Astronomy Department, University of Nevada, Las Vegas, 4505 S. Maryland Parkway, Las Vegas, NV 89154-4002, USA
[2] Department of Physics, The Citadel, 3 Jenkins Avenue, Grimsley Hall, Room 202, Charleston, SC 29409, USA
*Received 2019 October 11; accepted 2019 December 16; published 2020 January 13*

## Abstract

We have discovered period decreases for the mCP Si stars 13 And and V913 Sco from analyzing Strömgren *uvby* observations obtained with the Four College Automated Photometric Telescope at the Fairborn Observatory (FCAPT). We also have incorporated previously unpublished FCAPT data in further analyses of V901 Ori, CS Vir, and EE Dra for which other investigators have reported period changes. We confirm the results for V901 Ori but find no evidence for period change in CS Vir or EE Dra. It is impossible to distinguish between discrete period change models and linear change models for these stars from the available data; this also applies to CU Vir. We discuss some possible causes of this behavior.

*Key words:* stars: chemically peculiar – techniques: photometric

*Online material:* supplementary file

## 1. Introduction

When spectral classification was first performed about 100 yr ago at resolutions similar to that of the Henry Draper Catalog, some B- and A-type stars were found to not quite fit into the standard classification structure and were called peculiar. Many showed additional spectral lines and were later found to have strong global magnetic fields. Further observations showed that many of these stars exhibited spectral, magnetic and/or photometric variability. In stars where they could be measured, these changes all varied with the same period. This led to the development of the Oblique (or Rigid) Rotator Theory (e.g., see Stibbs 1950), whereby all the variations were attributed to the rigid rotation of the star. Later work involving considerably more data (e.g., Pyper et al. 1998; Mikulášek et al. 2008; Mikulášek 2016) revealed that in some cases these periods of variability changed with time. This paper discusses six stars for which we have obtained *uvby* photometry with the Four College Automatic Photometric Telescope (FCAPT); three of these stars have previous publications indicating that their periods are variable.

## 2. Observations

Table 1 contains information for the observed stars from Hoffleit (1982), Hoffleit et al. (1983), and the SIMBAD database. Included are the number of data points, the time interval over which the star was observed and the observer. The FCAPT method of observations is outlined in several previous papers (e.g., Adelman 2006). The FCAPT operated from 1990 through 2013.

The FCAPT is an automated telescope without an onsite observer. Thus, the users of its data must be especially careful about which data to keep. Data from groups which were not completely observed were not analyzed. In a group, if any of the standard deviations of the comparison-check star values exceeded 2% of the average values we excluded all the observations of a group so affected following Strassmeier & Hall (1988). Still, light curve inspections showed some obvious outliers. In these cases, we compared the difference between the value of an apparent outlier and the value of the fit at a given phase to the standard deviation of the fit. If a point is more than 3 standard deviations from the fit in any filter, then all the values in its group are removed from the data sets of all filters.

## 3. Period Analysis

All the stars discussed in this paper have previously published periods. We did a preliminary check of 87 mCP stars that were observed with the FCAPT for possible period changes. For stars that had good previously published data sets, we determined the periods that best matched these data and the FCAPT data. In most cases, the FCAPT photometry best defines the light curves and have been used to improve the estimated precision of the periods. To estimate precision, we used the practical method of comparing the two good data sets most widely separated in time and determined how much the period had to be changed in order to see a definite shift in phase. The FCAPT photometric data are in Tables A1–A5, which are included as a supplement to this paper.

**Table 1**
Photometric Groups

| HD | HR | Name | Type | $V$ | Spectral Type | Filter | No. | Interval | Observer |
|---|---|---|---|---|---|---|---|---|---|
| 37776 | | V901 Ori | v | 6.96 | B2IV/V-s | 1 | 375 | 1994–2013 | A |
| 36591 | 1861 | | c | 5.35 | B1IV | 3 | | | |
| 40574 | 2109 | | ch | 6.63 | B8IIIn | 2 | | | |
| 125248 | 5355 | CS Vir | v | 5.90 | A0pCrEu | 2 | 318 | 1990–2007 | AP |
| 124683 | 5332 | | c | 5.43 | A0 | 2 | | | |
| 125048 | | | ch | 6.90 | A3V | 2 | | | |
| 142990 | 5942 | V913 Sco | v | 5.43 | B5IV-w | 3 | 368 | 1992–2005 | AP |
| 142165 | 5906 | | c | 5.39 | B6IVn | 3 | | | |
| 142114 | 5904 | 2 Sco | ch | 4.59 | B2.5V | 3 | | | |
| 177410 | 7224 | EE Dra | v | 6.52 | A0pSi | 1 | 820 | 1993–2013 | A |
| 179933 | 7290 | 55 Dra | c | 6.16 | A0V | 1 | | | |
| 182564 | 7371 | $\pi$Dra | ch | 4.59 | A2IIIs | 3 | | | |
| 220885 | 8913 | 13 And | v | 5.75 | B9III | 2 | 89 | 2001–2013 | A |
| 222109 | 8962 | | c | 5.80 | B8V | 2 | | | |
| 221756 | 8947 | 15 And | ch | 5.59 | A1III | 2 | | | |

**Note.** (1) Type of star: v = variable star, c = comparison star, ch = check star. (2) Filters: 1 = no neutral density filter, 2 = 1.25 mag. Neutral density filter, and 3 = 2.50 mag. Neutral density filter. (3) No. = Number of good observations. (4) Observer: A = Adelman, P = Pyper.

**Table 2**
Data Quality Assessment for V901 ORI Data Sets

| DQ | Scatter (1) | Phase Coverage |
|---|---|---|
| 1 | 15% | complete |
| 2 | 30% | complete or small gaps |
| 3 | 50% | complete |
| 4 | 70%–80% | complete or gaps |
| 5 | $\geqslant$Ampl. | variation not detectable |

**Note.** (1) Approximate percentage of the amplitude of light variation.

Any changes in the periods appear as shifts in the phases of the light curves. Besides CU Vir, whose period changes had already been detected (Pyper et al. 1998, 2013), we found such phase shifts for V901 Ori, V913 Sco and 13 And, but not for CS Vir or EE Dra. To further characterize the period changes, we used $O - C$ analysis for the best photometry. As was done in the two CU Vir papers, we plot

$$O - C = \mathrm{JD} - (\mathrm{JD}_0 + P_0\, \boldsymbol{E}), \tag{1}$$

where JD represents the Heliocentric Julian Date of the maximum or minimum determined from the fit to the light curve over a given observation period and $\boldsymbol{E}$ is the nearest whole value to $E_{\rm calc} = (\mathrm{JD} - \mathrm{JD}_0)/P_0$; $\mathrm{JD}_0$ and $P_0$ refer to an ephemeris selected by the authors for the comparison. As for CU Vir, the maxima or minima of the light curves were determined from curve fits to a five parameter Fourier series. In $O - C$ versus $E$ plots, a discrete period change is indicated by an abrupt change in slope, where the new slope is $P_0 + \Delta P$ and $\Delta P$ is a constant. A linear period change is indicated by a curved line, represented by a 2nd order polynomial (parabola),

$$O - C = a + bE + cE^2. \tag{2}$$

The coordinates of the maximum or minimum of this 2nd order polynomial are $E_m$ and $(O - C)_m$, where $E_m = -b/2c$, and $(O - C)_m$ is determined from Equation (2), with $E = E_m$. The corresponding values of $\mathrm{JD}_m$ and $P_m$ for this minimum are $\mathrm{JD}_m = a + \mathrm{JD}_0$ and $P_m = b + P_0$. The rate of change in the period in days per cycle is $\alpha = 2c$ (this is the constant rate of change of the slope of the tangent to the parabola). Where available, we also examined the variations of the magnetic field and spectrum as supplements to the photometric data. It should be noted that in all the subsequent sections, JD signifies the Heliocentic Julian Date.

## 4. Analysis of Observations

In the following subsections we examine for period changes five stars for which we have FCAPT observations that have not been reported in the literature. When they extend previously published FCAPT observations we combine both sets of data. When comparing photometric data sets, we made appropriate normalizations to the same magnitude range. In Section 5 we reexamine the data for CU Vir, for which we have published all our FCAPT observations. In discussing the longitudinal magnetic fields of these stars, we note that there are three different ways of measuring them, using Zeeman analyzers, H$\alpha$ photometry and Stokes parameters. All give similar results although there are usually shifts between them. Nowadays, $Bz$ is

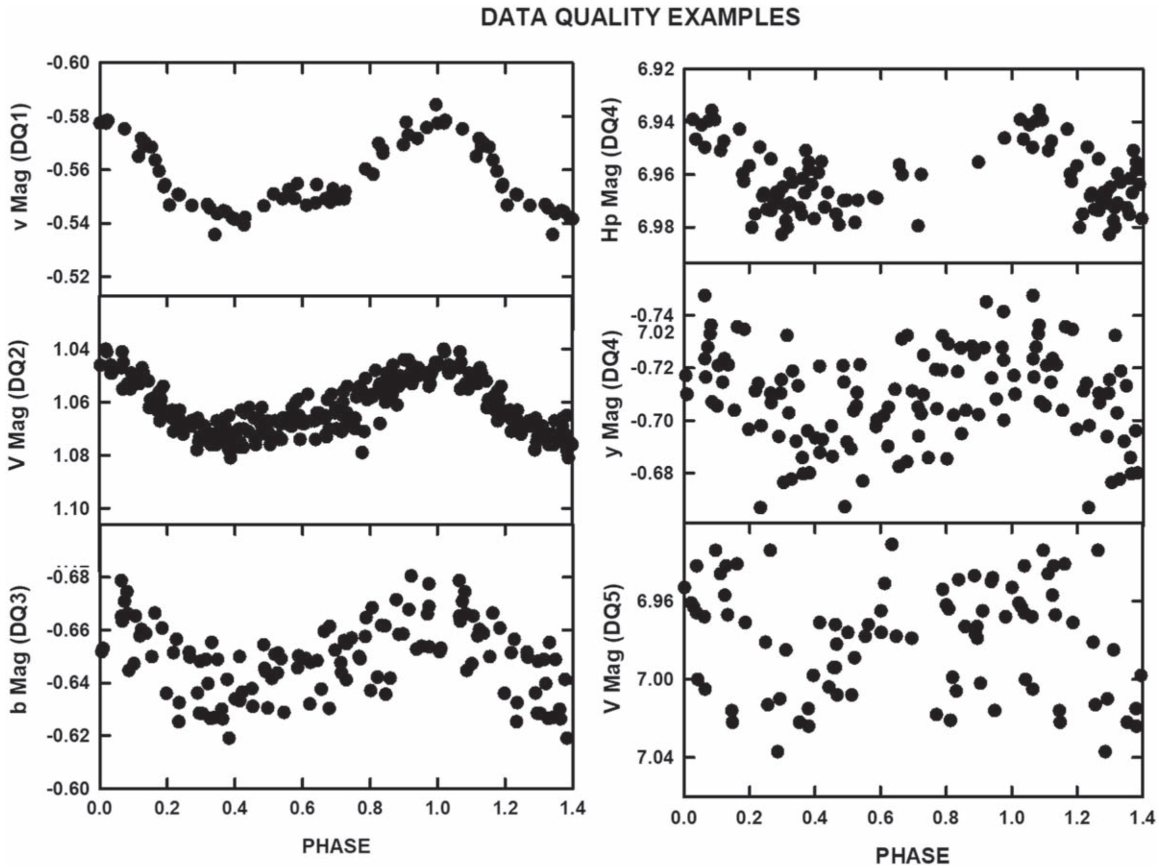


**Figure 1.** Examples of the DQ classes summarized in Table 3. Phases are calculated from the ephemeris JD = 2456256.940 + 1.538775 *E*. All are the same scale except the DQ5 plot.

usually used to represent the longitudinal magnetic field and we use this symbol throughout the paper.

### 4.1. V901 Ori = HD 37776

Adelman (1997) determined a period of 1.538675 days for V901 Ori by comparing FCAPT data from 1994–96 with previously published data. This star was first determined to have an increasing period by Mikulášek et al. (2008). The unpublished FCAPT photometry of V901 Ori from 2004–2013 is included in Table A1. The amplitudes of variation ($a$) of V901 Ori are relatively small; $a \approx 0.03$ mag for most filters. The magnitude of this star is also relatively faint, so the available photometric data are much affected by scatter and therefore the data sets vary in quality. To determine which data sets to use in the $O - C$ analysis, we examined each year of our FCAPT data and the photometric data sets used by Mikulášek and his collaborators in their 2008 and 2011 papers. We assigned a data quality index DQ based on visual inspection of the light curves; criteria for this index are summarized in Table 2. Figure 1 shows example plots of each category. It was clear that neither DQ class 4 or 5 would be useful in the analysis and that class 1 and 2 should be included.

Table 3 summarizes the DQ information for all the photometry data sets. For the data sets classified as DQ = 3, we used visual examination of the light curves in comparison with the other included data to determine whether they should be used in the analysis. In the Comments, the observatories listed (3, 4 and 5) are identified in Mikulášek et al. (2008). Data sets with less than 17 points were not used in the analysis.

Figure 2 shows the *uvby* light curves for Data Sets (DS) 15a–23a having DQ = 1. Also included are the *BV* light curves for DS6a. We also plotted the *v* values for DS1a to show the phase shift due to the period change. The DS5a *Hp* values are plotted with the *b* values and the DS12a *V* values are plotted with the *V* values of DS6a for comparison.

The $O - C$ plot for V901 Ori is shown in Figure 3, where $JD_0$ and $P_0$ are from the ephemeris of Pedersen & Thomsen (1977), ($O - C = \mathrm{JD} - 2442780.785 + 1.53863\,E$). The $O - C$ values for all the filters that were used (Table 3) for each data set are plotted. Although it was not used in the analysis, the *Hipparcos Hp* data (DS5a) is also plotted. The

**Table 3**
Photometric Data Sets for V901 ORI

| Set No. | Yrs Obs | No. | DQ | Comments | Used? | References |
|---|---|---|---|---|---|---|
| 1a | 1976 | 54 | 1 | | Y *uvby* | Pedersen & Thomsen (1977) |
| 2a | 1977–78 | 58 | 4-5 | 1 | N *UiBiVi* | Bartolini et al. (1982) |
| 3a | 1979–84 | 18 | 2 | | Y *uvby* | Adelman & Pyper (1985) |
| 4a | 1990 | 41 | 4 | | N *Hp* | *Hipparcos* (ESA 1997) |
| 5a | 1991–92 | 122 | 4 | | N *Hp* | *Hipparcos* (ESA 1997) |
| 6a | 2006–07 | 216 | 1–2 | 2, 3 | Y *BV* | Mikulášek et al. (2008) |
| 7a | 2009–10 | 185 | 2 | 2, 3 | Y *BV* | Mikulášek et al. (2011) |
| 8a | 2006–07 | 44 | 4 | 2, 4 | N *UBV* | Mikulášek et al. (2008) |
| 9a | 2000–01 | 15 | 4 | 2, 5 | N *V* | Mikulášek et al. (2008) |
| 10a | 2001–02 | 13 | 4 | 2, 5 | N *V* | Mikulášek et al. (2008) |
| 11a | 2002–03 | 39 | 4 | 2, 5 | N *V* | Mikulášek et al. (2008) |
| 12a | 2003–04 | 75 | 2 | 2, 5 | Y *V* | Mikulášek et al. (2008) |
| 13a | 2004–08 | 203 | 5 | 2, 5 | N *V* | Mikulášek et al. (2008) |
| 14a | 2008–09 | 48 | 4 | 2, 5 | N *V* | Mikulášek et al. (2008) |
| 15a | 1994–95 | 21 | 1 | | Y *uvby* | FCAPT, Adelman (1997) |
| 16a | 1995–96 | 22 | 1 | | Y *uvby* | FCAPT, Adelman (1997) |
| 17a | 2004–05 | 11 | 4 | | N *uvby* | FCAPT, this paper |
| 18a | 2006–07 | 43 | 2 | | Y *uvby* | FCAPT, this paper |
| 19a | 2008–09 | 26 | 1–3 | | Y *uvby* | FCAPT, this paper |
| 20a | 2009–10 | 67 | 4–5 | | N *uvby* | FCAPT, this paper |
| 21a | 2010–11 | 94 | 3–4 | 6 | Y *uvb* N *y* | FCAPT, this paper |
| 22a | 2011–12 | 35 | 1–4 | 6 | Y *uvb* N *y* | FCAPT, this paper |
| 23a | 2012–13 | 56 | 1 | | Y *uvby* | FCAPT, this paper |

**Note.** (1) No. = Number of data points, (2) DQ = Data quality, (3) Y = Yes, (4) N = No, (5) Comments: 1: Instrumental magnitudes; 2: Data available in the "mCP Online Database" (http://astro.physics.muni.cz/mcpod/); 3: Fairborn Observatory; 4: Hvar Observatory; 5: All Sky Automated Survey (ASAS); 6: DQ = 4 for *y*.

measurement errors for DS5a (0.10) and DS12a (0.06) were estimated from the uncertainty in the determination of the light curve maxima from the plots. The $O-C$ data (including *Hipparcos*) are consistent with two models. Model 1 (M1): a constant period $P_1 = 1.53863$ days until 1989, then an abrupt increase to a constant period $P_2 = 1.538774$ days from 1989 to 2013; and Model 2 (M2): a linear increase in the period over the entire time span of the measurements, with $\mathrm{JD}_m = 2442780.774$ and $P_m = 1.538630$ days (see Equation (2)). Note that in this model, $P_m = P_1$ of M1. A third model, M3, is also possible, with a constant period of 1.53863 days until 1983, a discrete period change to a constant period of 1.538699 days until 1998 and another discrete change to a constant period of 1.538791 until at least 2013; as far as the data are concerned, it is not possible to distinguish between M2 and M3. Our $O-C$ results show for M1 an increase in the period of 12.5 s and for M2 an increase of 16.7 s from 1977–2013 where $\alpha = 2.21 \times 10^{-8}$ days per cycle or 455 ms $\mathrm{yr}^{-1}$. The latter value is somewhat larger than the results of Mikulášek (2016) who assumed a linear change in the period and found an increase of 350 ms $\mathrm{yr}^{-1}$. This discrepancy may be due to the fact that we only used the best photometry in our analysis whereas Mikulášek used all the photometry as well as the magnetic and spectral data.

The question remains as to whether the available data better agree with M1 or M2. The photometric data do not help in this respect, since there are no observations in the interval 1985–1990, where the two models differ the most. We also examined the magnetic and spectrum variations of V901 Ori in hopes that they might help distinguish between the models. Table 4 summarizes the published data for these quantities. Due to the complexity of these variations and the lack of complete phase coverage in most of the data sets, we examined the plots of variation versus phase for the magnetic field and He I variations. The Si IV and C IV data were not used since they vary in antiphase to He I and show large scatter.

Unfortunately, there are no magnetic or spectrum measurements between 1986 and 1990 so there is still no clear distinction between M1 and M2. However, in Figure 4 we plotted the magnetic and spectrum variations to see if the plots better agree with one model over the other. The most complete phase coverage for the magnetic field is found in DS28a (see Table 4); DS26a and 30a have small numbers of data points; all three data sets are plotted in Figure 4. In Figure 4(a) we assume M1, where $P_1$ is the period of DS26a and 28a and $P_2$ is the period of DS30a. Phase shifts appropriate to the difference in periods have been subtracted from the DS30a data. In Figure 4(b) we assume M2; a period $P_{cc}$ has been calculated for each data set,

$$P_{cc} = P_m + \alpha(E - E_m), \tag{3}$$

where $P_m$ and $\alpha$ are defined in Equation (2), $E_m$ is the epoch of $P_m$ and $E$ is the median epoch for each data set. In the case of

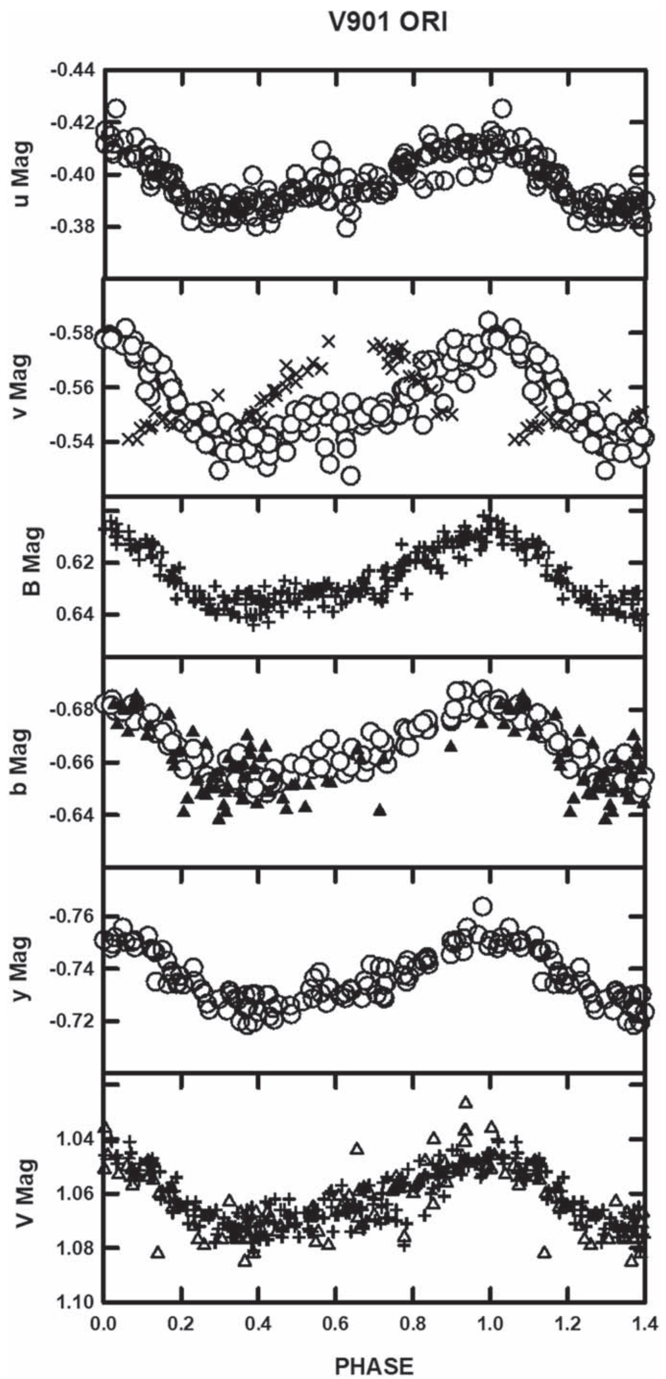


**Figure 2.** Photometric light curves for V901 Ori. Open circles are the FCAPT data (DS15a-23a), pluses are the DS6a data, crosses are the DS1a data, closed triangles are the DS5a data and open triangles are the DS12a data. Phases are calculated with the same ephemeris as in Figure 1.

the 2nd order polynomial fit for the $O - C$ plot of V901 Ori, $P_m = P_1$ and $E_m = 0$, so $P_{cc} = P_1 + \alpha E$. As for M1, we subtracted appropriate phase shifts to each data set to reduce them to the phase for $P_1$.

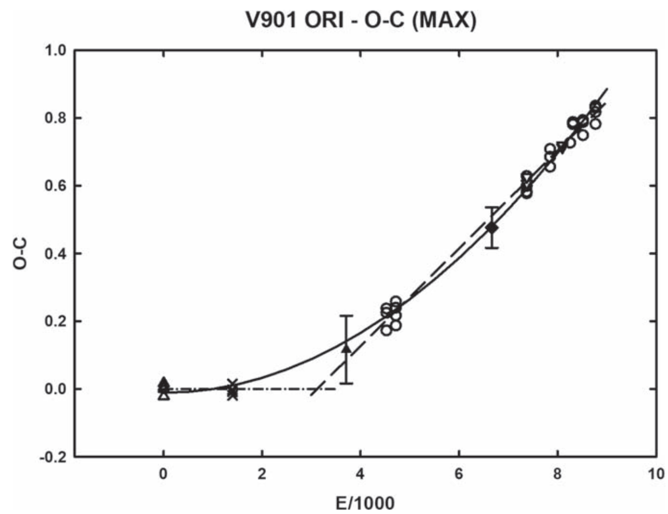


**Figure 3.** $O - C$ diagram of V901 Ori for the data sets used (see Table 3). The solid curve is a 2nd order polynomial fit to all the data, the dotted–dashed line represents $P_1$ and the dashed line is the linear fit to data sets after 1994. The open circles are the FCAPT data (DS15a-23a), the open triangles and crosses are DS1a and 3a, the filled triangle is DS5a, the open inverse triangles are DS6a and 7a, the closed diamond is DS12a. The estimated measurement errors for DS5a and DS12a are indicated on the plot.

We applied the same techniques to the He I variations. DS24a and 25a use $R$, a photometric index to measure the strength of the He I $\lambda$4026 line, which is plotted in Figure 4(c). Mikulášek et al. (2008) also published equivalent widths ($W_\lambda$) for a number of He I lines obtained with the Canada–France–Hawaii Telescope (CFHT) and at the Special Astrophysical Observatory (SAO). To generate DS29a, 30a and 32a, we were able to determine the median equivalent widths ($\langle W \rangle$) for six He I lines (see Table 4) and determine averages of the quantity $W_\lambda / \langle W \rangle$ for each data set. We then averaged these quantities to generate the data plotted in Figures 4(d) and (e) (Table 5).

In Figure 4(d), we assumed $P_1$ to be the period of DS24a, 25a and 29a and $P_2$ to be the period of DS31a and 32a. For Figure 4(e), we determined $P_{cc}$ in the same way as in Figure 4(b). Although the M1 plots (Figures 4(a) and (d)) show slightly better agreement than do the M2 plots (Figures 4(b) and (e)), again we cannot clearly distinguish between the models. This is especially true of the magnetic field measurements, since most of the published errors of these values are between ±200 G and ±400 G. Overall, considering both the photometry and the magnetic and spectrum variations, we conclude that neither a linear nor a discrete period change can be ruled out for V901 Ori. We also find that the $O - C$ diagram does not show a decrease in the period through 2013. Mikulášek et al. (2011) predicted a possible halt to the increase in 2003 but this is not confirmed by the more recent data.

**Table 4**
Magnetic Field and Spectrum Variation Data for V901 ORI

| Set No. | Yrs Obs | No. | Data Type | Comments | Plotted? | References |
|---|---|---|---|---|---|---|
| 24a | 1976 | 37 | *R*: He I 4026 | | Y | Pedersen & Thomsen (1977) |
| 25a | 1976 | 16 | *R*: He I 4026 | | Y | Pedersen (1979) |
| 26a | 1978 | 7 | MF | | Y | Borra & Landstreet (1979) |
| 27a | 1980 | 16 | *a*: Si IV, C IV | 1 | N | Shore & Brown (1990) |
| 28a | 1982–84 | 37 | MF | | Y | Thompson & Landstreet (1985) |
| 29a | 1986 | 13 | $W_\lambda$: He I | 2, 3 | Y | Mikulášek et al. (2008) |
| 30a | 1993 | 5 | MF | | Y | Donati et al. (1997) |
| 31a | 1994–96 | 25 | $W_\lambda$: He I 4471, 5875 | 4 | Y | Mikulášek et al. (2008) |
| 32a | 2000–02 | 6 | $W_\lambda$: He I 4471 | 4 | Y | Mikulášek et al. (2008) |

**Note.** (1) No. = Number of data points, (2) $R$ = Photometric index (see text), (3) MF = Magnetic field, (4) $a$ = Line strength index, (5) $W_\lambda$ = Equivalent width, (6) Y = Yes, (7) N = No, (8) Comments: 1: Large scatter; 2: CFHT data; 3: Data for He I $\lambda\lambda$4013, 4120, 4143, 4168, 4471, 5875; 4: SAO data.

**Table 5**
Normalized He I Equivalent Widths for V901 ORI

| Set No. | HJD | PH M1 | PH M2 | $W_\lambda/\langle W\rangle$ | Set No. | HJD | PH M1 | PH M2 | $W_\lambda/\langle W\rangle$ |
|---|---|---|---|---|---|---|---|---|---|
| 29a | 2446450.854 | 0.288 | 0.247 | 1.184 | 31a | 2449736.326 | 0.535 | 0.452 | 1.000 |
| 29a | 2446451.027 | 0.400 | 0.359 | 1.207 | 31a | 2449738.262 | 0.793 | 0.710 | 1.150 |
| 29a | 2446451.748 | 0.869 | 0.828 | 0.978 | 31a | 2449788.184 | 0.239 | 0.156 | 0.961 |
| 29a | 2446451.829 | 0.921 | 0.880 | 0.924 | 31a | 2449788.208 | 0.255 | 0.172 | 0.900 |
| 29a | 2446451.958 | 0.005 | 0.964 | 0.814 | 31a | 2450056.527 | 0.643 | 0.560 | 1.073 |
| 29a | 2446452.743 | 0.515 | 0.474 | 1.112 | 31a | 2450056.544 | 0.654 | 0.571 | 1.094 |
| 29a | 2446452.903 | 0.619 | 0.578 | 1.109 | 31a | 2450057.286 | 0.136 | 0.053 | 0.784 |
| 29a | 2446452.981 | 0.670 | 0.629 | 1.206 | 31a | 2450057.308 | 0.151 | 0.068 | 0.916 |
| 29a | 2446453.711 | 0.145 | 0.104 | 0.814 | 31a | 2450057.486 | 0.266 | 0.183 | 1.010 |
| 29a | 2446453.881 | 0.255 | 0.214 | 1.030 | 31a | 2450057.508 | 0.281 | 0.198 | 1.081 |
| 29a | 2446453.937 | 0.291 | 0.250 | 1.172 | 31a | 2450059.388 | 0.502 | 0.419 | 1.216 |
| 29a | 2446453.983 | 0.321 | 0.280 | 1.182 | 31a | 2450059.412 | 0.518 | 0.435 | 1.134 |
| 29a | 2446454.012 | 0.340 | 0.299 | 1.174 | 31a | 2450060.302 | 0.097 | 0.014 | 0.816 |
| 29a | 2446450.806 | 0.257 | 0.216 | 1.191 | 31a | 2450060.324 | 0.111 | 0.028 | 0.732 |
| 29a | 2446450.946 | 0.348 | 0.307 | 1.175 | 31a | 2450060.524 | 0.241 | 0.158 | 0.975 |
| 29a | 2446451.776 | 0.887 | 0.846 | 0.963 | 31a | 2450060.546 | 0.255 | 0.172 | 1.045 |
| 29a | 2446451.904 | 0.970 | 0.929 | 0.834 | 31a | 2450500.252 | 0.033 | 0.950 | 1.017 |
| 29a | 2446452.016 | 0.043 | 0.002 | 0.729 | 31a | 2450681.558 | 0.869 | 0.786 | 1.010 |
| 29a | 2446452.712 | 0.495 | 0.454 | 1.080 | 31a | 2450707.472 | 0.711 | 0.628 | 1.145 |
| 29a | 2446452.821 | 0.566 | 0.525 | 1.099 | 31a | 2450709.550 | 0.062 | 0.979 | 0.855 |
| 29a | 2446453.766 | 0.180 | 0.139 | 0.914 | 31a | 2450710.490 | 0.673 | 0.590 | 1.030 |
| 29a | 2446453.937 | 0.291 | 0.250 | 1.124 | 32a | 2451799.564 | 0.424 | 0.295 | 1.108 |
| 29a | 2446454.774 | 0.835 | 0.794 | 0.892 | 32a | 2451799.583 | 0.437 | 0.308 | 1.091 |
| 31a | 2449641.469 | 0.885 | 0.802 | 0.988 | 32a | 2452333.158 | 0.223 | 0.094 | 0.876 |
| 31a | 2449641.601 | 0.970 | 0.887 | 0.846 | 32a | 2452333.174 | 0.233 | 0.104 | 0.958 |
| 31a | 2449642.425 | 0.506 | 0.423 | 1.077 | 32a | 2452333.190 | 0.243 | 0.114 | 1.078 |
| 31a | 2449736.303 | 0.520 | 0.437 | 1.092 | 32a | 2452333.220 | 0.263 | 0.134 | 1.020 |

**Note.** (1) Set No. is from Tables 4, (2) PH M1 and PH M2 are phases from M1 and M2 (see text), (3) $W_\lambda$ = Equivalent width.

### 4.2. *CS Vir = HD 125248*

Recently, Ozuyar et al. (2018) (hereafter designated as OSS), report that they found a period increase of 660 ms yr$^{-1}$ for CS Vir based on data from the *Solar Terrestrial Relations Observatory* (*STEREO*) satellite from 2007–2011 compared with previously published photometric and spectral data. We obtained FCAPT *uvby* data for CS Vir from 1990–2007 (Table 1, Table A2) which have not yet been published. Since OSS did not have access to our FCAPT data for this star, we reanalyzed all the photometric data available, summarized in Table 6. We did not use data sets with $N < 20$ in the analysis (DS3b, 6b, 7b,10b) or the spectrum or magnetic data sets

(Table 7). As we did for V109 Ori, we plotted an $O-C$ diagram (Figure 5) including all the data sets indicated as "Y" in Table 6, with $JD_0 = 2440382.25$ and $P_0 = 9.2954$ (see Equation (1)). As Equation (1) shows, $O-C$ is proportional to the period, and so small uncertainties in the determination of the phase of maximum light will lead to relatively large shifts in the $O-C$ values for a star with a long period, such as CS Vir. Figure 6 shows that the shapes and amplitudes of the light curves change depending on the filter used. We used the $u$, $U$, $v$, and $B$ data in the analysis, since they have the largest amplitudes and the best-determined light curves; they also most closely match the photometry of Stibbs (DS1b) and OSS. (DS18–22b), both of which have effective wavelengths of approximately 4000 Å. The data points in Figure 5 are averages of $U$ and $B$ for the Johnson photometry and $u$ and $v$ for the Strömgren photometry. The $JD_{max}$ values used to calculate $E$ and $O-C$ for DS18b–22b were taken from OSS; also included is the $JD_{max}$ $U$ value of Blanco et al. (1978) listed in OSS (the star in Figure 5). Since Stibbs (DS1b) used only one filter; the measurement error, shown by the bar in Figure 5, was estimated from the uncertainty in the determination of the light curve maxima from the plots; due to this uncertainty, this data set was also not included in the analysis. The remaining data fit a linear regression ($R^2 = 0.91$), indicating $P = 9.29553$ days, which is the same as the period determined from comparison of the light curves of the FCAPT data, $P = 9.29548 \pm 0.00008$ days. If a 2nd order polynomial is fit to the data points including DS1b, a linear period increase of 160 ms $yr^{-1}$ ($R^2 = 0.93$) results (dashed line in Figure 5) but this is not detectable by comparing the light curves or magnetic field variations.

We were puzzled to see how OSS found such a large change, 660 ms $yr^{-1}$, in the period of CS Vir. If the FCAPT data are removed from Figure 5, and only the $u$ and $U$ values are used for the rest of the photometry, the $O-C$ plot can be fit by a 2nd order polynomial indicating a linear period increase of 390 ms $yr^{-1}$ (solid curve in Figure 5). If we use the data published by OSS for only the photometry, we find an increase of 360 ms $yr^{-1}$, which is essentially the same as our result. If the line intensity data of Deutsch (1947), published by OSS, is added to the rest of the OSS data the period increase changes to 620 ms $yr^{-1}$, so it appears that the Deutsch data are mainly responsible for the change reported by OSS. We were surprised that the Deutsch data were given such a large weight, since the plots show large scatter. We also noted that the "Corrected Maximum Time" listed by OSS for the Deutsch data is JD = 2430148.187, which is 5.117 days + $JD_0$ = 2430143.07, the latter being of the time of maximum line intensity estimated by Deutsch, but one would expect the corrected JD to be

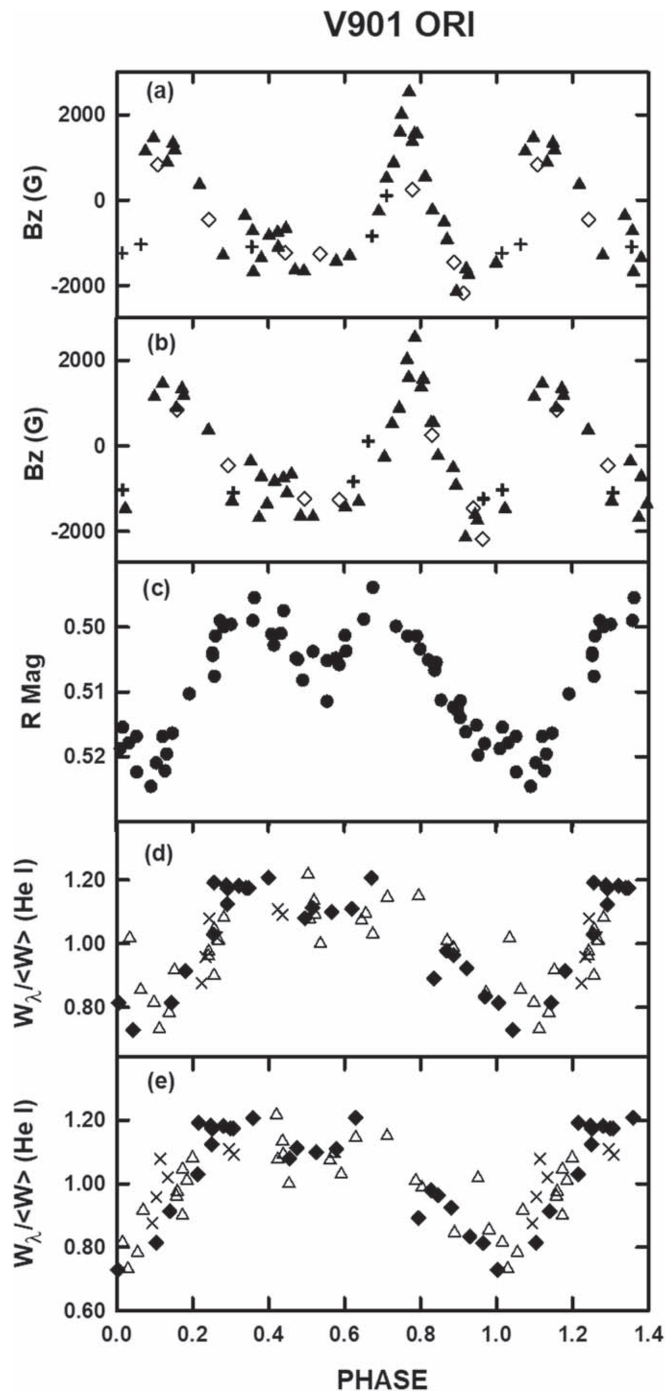


**Figure 4.** Magnetic and He I spectrum variations of V901 Ori. In (a) and, (b), open diamonds, filled triangles and pluses represent DS26a, 28a and 30a, respectively; in (c), filled circles represent DS24a and 25a; in (d) and (e), closed diamonds, open triangles and crosses represent DS29a, 31a and 32a, respectively. Phases are calculated from the ephemeris JD = 2442780.785 + 1.53863 $E$ ($P_1$). Appropriate phase shifts were applied to DS 29a, 30A, 31a and 32a (see text).

**Table 6**
Photometry Data Sets for CS VIR

| Set No. | Yrs Obs | No. | Comments | Used? | References |
|---|---|---|---|---|---|
| 1b | 1949 | 26 | 1 | N mi | Stibbs (1950) |
| 2b | 1969 | 28 | | Y *UB* N *V* | Maitzen & Rakosch (1970) |
| 3b | 1970 | 13 | | N *uvby* | Wolff & Wolff (1971) |
| 4b | 1970–71 | 31 | | Y *uv* N *by* | Maitzen & Moffat (1972) |
| 5b | 1970–71 | 57 | | Y *UB* N *V* | Maitzen & Moffat (1972) |
| 6b | 1983–85 | 13 | | N *uvby* | Pyper & Adelman (1985) |
| 7b | 1991 | 10 | | N *uvby* | Catalano et al. (1992) |
| 8b | 1990–92 | 81 | 1 | N *Hp* | *Hipparcos* (ESA 1997) |
| 9b | 1990–91 | 21 | | Y *uv* N *by* | FCAPT this paper |
| 10b | 1991–92 | 10 | | N *uvby* | FCAPT this paper |
| 11b | 1992–93 | 58 | | Y *uv* N *by* | FCAPT this paper |
| 12b | 1993–94 | 26 | | Y *uv* N *by* | FCAPT this paper |
| 13b | 1994–95 | 26 | | Y *uv* N *by* | FCAPT this paper |
| 14b | 1995–96 | 52 | | Y *uv* N *by* | FCAPT this paper |
| 15b | 1999–2000 | 30 | | Y *uv* N *by* | FCAPT this paper |
| 16b | 2005–06 | 46 | | Y *uv* N *by* | FCAPT this paper |
| 17b | 2006–07 | 48 | | Y *uv* N *by* | FCAPT this paper |
| 18b | 2007 | 638 | 2 | Y mc | Ozuyar et al. (2018) |
| 19b | 2008 | 587 | 2 | Y mc | Ozuyar et al. (2018) |
| 20b | 2009 | 249 | 2 | Y mc | Ozuyar et al. (2018) |
| 21b | 2010 | 605 | 2 | Y mc | Ozuyar et al. (2018) |
| 22b | 2011 | 633 | 2 | Y mc | Ozuyar et al. (2018) |

**Note.** (1) No. = Number of data points, (2) Y = Yes, (3) N = No, (4) mi = instrumental magnitude: $\lambda_{\rm eff} \sim 4000$ Å, (5) mc = instrumental magnitude: $\lambda_{\rm eff} \sim 4000$ Å, (6) Comments: 1: only single filter; 2: HI-1A Camera.

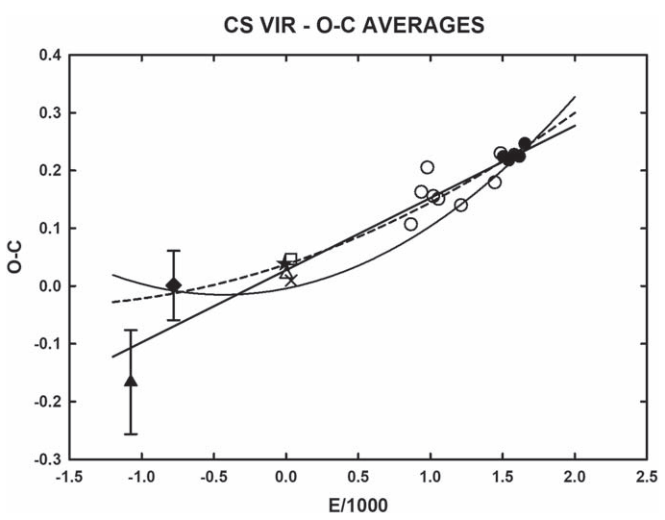


**Figure 5.** $O - C$ diagram for CS Vir. Filled diamond, closed triangle, cross, and open square are DS1b, 2b, 4b, and 5b, respectively. Open circles are the FCAPT data (DS9b, DS11b-17b) and closed circles are the OSS data (DS18b-22b). The solid line is the linear regression for DS3b-22b; the dashed curve is the 2nd order polynomial fit to all the photometric data listed as "Y" in Table 6, plus DS1b. The filled triangle (DS23b), star and solid curve are discussed in the text.

$\mathrm{JD}_0 + 4.65$ days, which is one-half Deutsch's estimated period of 9.295 days, assuming that the line intensity peaks at a phase of 0.5. Moreover, when we calculate the $O - C$ using $\mathrm{JD}_0$, we get $O - C = -0.297$, as opposed to $O - C = +0.173$ published by OSS using their corrected JDH. To clarify the situation, we replotted the data that Deutsch published, DS23b, for the average line intensities of three spectrum lines that vary synchronously ("Criterion V"), using the same ephemeris JD = 2440382.250 + 9.29548 $E$. that we used for all of the other data sets.

This plot, along with its curve fit, is shown in Figure 7, which illustrates comparisons of photometric, spectrum and magnetic data from 1941–2007 (the *STEREO* data of OSS are not currently available). We used the curve fit to determine the JD of maximum line intensity, which results in a value of $O - C = -0.166$. This value is plotted in Figure 5 along with its estimated measurement error; it is consistent with the linear regression determined from the photometry. Although Deutsch does not specify how he estimated his $\mathrm{JD}_0$ (2430143.07), it should be noted that if $\mathrm{JD}_0 = 2430143.17$ then $O - C = -0.197$, so there may have been an error in the publication of the $\mathrm{JD}_0$ value. It is unclear how OSS derived the correction they publish for the Deutsch data.

Although the addition of the FCAPT photometry and the recalculation of the Deutsch data do not support a period change in CS Vir, it would be useful if we could show no phase shifts in the plots of the available data. Table 7 summarizes the spectrum and magnetic field data for CS Vir. Unfortunately, the earliest data set, the line intensity data of Deutsch (DS23b) shows a large scatter (Figure 7). In his study of the

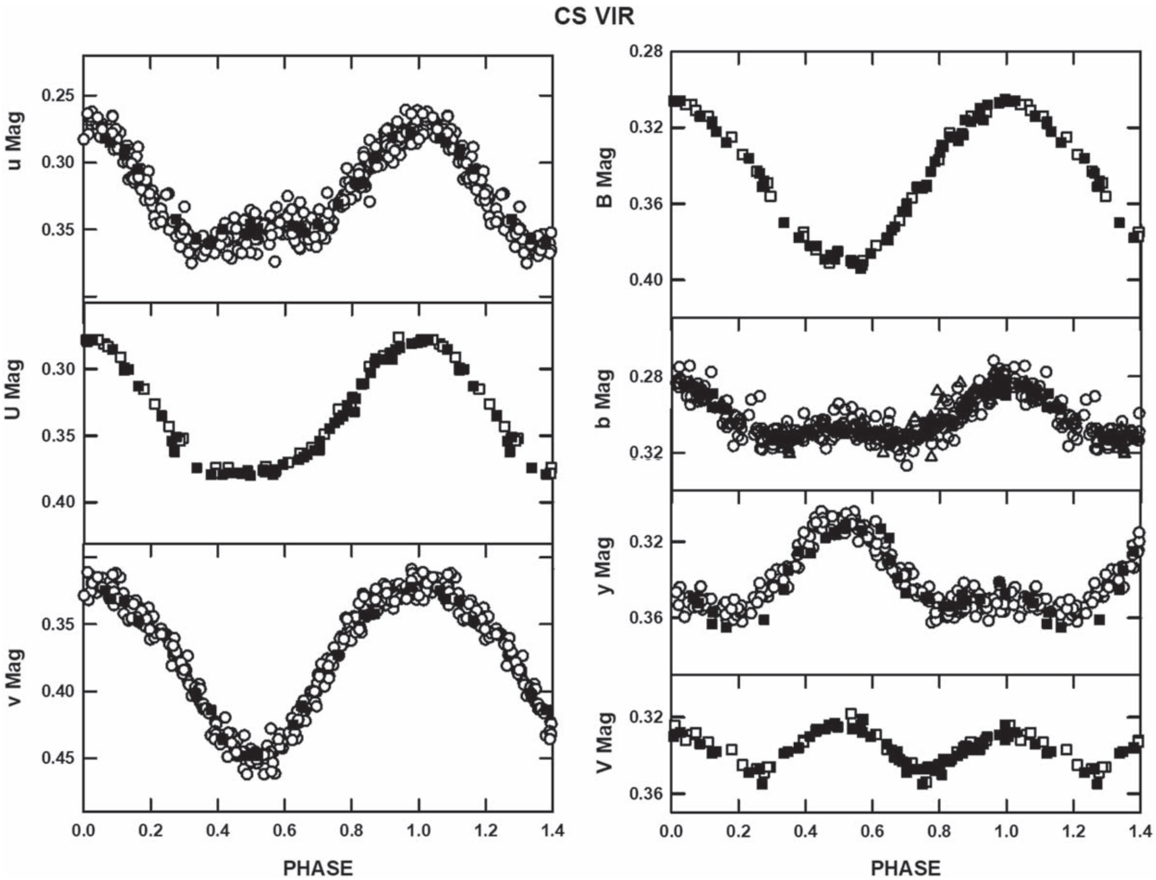


**Figure 6.** Photometric variations for CS Vir. Open circles represent the FCAPT data (DS9b-17b). Open squares, closed squares, and open triangles represent DS2b, DS4b-5b, and DS8b, respectively. All data are plotted with the ephemeris JD = 2440382.250 + 9.29548 *E*.

**Table 7**
Magnetic Field and Spectrum Data for CS VIR

| Set No. | Yrs Obs | No. | Type | Method | References |
|---|---|---|---|---|---|
| 23b | 1941–43 | 25 | Line Intensity | 1 | Deutsch (1947) |
| 24b | 1947–50 | 27 | Mag. Field | 2 | Babcock (1951) |
| 25b | 1953–57 | 11 | Mag. Field | 2 | Babcock (1958) |
| 26b | 1964 | 6 | Mag. Field | 2 | Adam (1965) |
| 27b | 1964–65 | 8 | Mag. Field | 2 | Hockey (1971) |
| 28b | 1975–78 | 15 | Mag. Field | 3 | Borra & Landstreet (1980) |
| 29b | 1970 | 1 | Mag. Field | 3 | Landstreet et al. (1975) |
| 30b | 1985–88 | 19 | Mag. Field | 4 | Mathys (1994) |
| 31b | 1992–93 | 2 | Mag. Field | 4 | Mathys & Hubrig (1997) |
| 32b | 1999 | 10 | Mag. Field | 4 | Leone & Catanzaro (2001) |
| 33b | 2001 | 9 | Mag. Field | 4 | Rusomarov et al. (2016) |
| 34b | 2012 | 12 | Mag. Field | 4 | Rusomarov et al. (2016) |

**Note.** (1) No. = Number of data points, (2) Method: 1: Visual estimate; 2: Zeeman analysis; 3: H$\alpha$; 4: Stokes parameters.

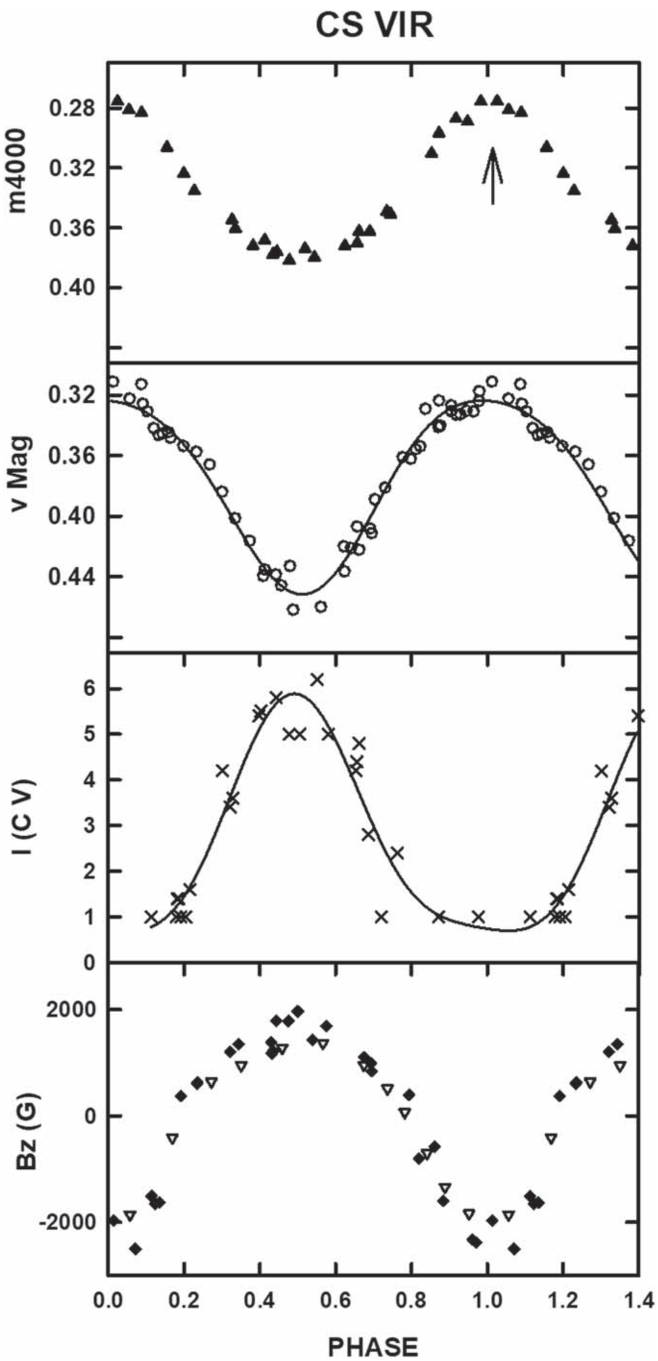


**Figure 7.** Photometric, spectrum and magnetic variations of CS Vir. For the photometric data, closed triangles are DS1b, and open circles are DS17b. Crosses represent the DS23b data (Table 7). For the magnetic field ($Bz$) data, closed diamonds and open inverse triangles are DS24b and DS34b, respectively. The solid curves in the $v$ plot and $I$ (C V) plot are the curve fits for DS 17b and DS23b, respectively. The arrow in the m4000 plot indicates the phase of light maximum for DS22b. All data are plotted with the same ephemeris as in Figure 6.

**Table 8**
Magnetic Field Data for CS VIR

| Set No. | HJD | Phase | $Bz$ |
|---|---|---|---|
| 24b | 2432364.668 | 0.475 | 2335 |
| 24b | 2432282.872 | 0.676 | 1650 |
| 24b | 2432317.821 | 0.435 | 1773 |
| 24b | 2432337.712 | 0.575 | 2245 |
| 24b | 2432366.713 | 0.695 | 1391 |
| 24b | 2432398.688 | 0.135 | −1077 |
| 24b | 2432399.617 | 0.235 | 1183 |
| 24b | 2432602.992 | 0.114 | −955 |
| 24b | 2432654.858 | 0.694 | 1547 |
| 24b | 2432655.787 | 0.794 | 949 |
| 24b | 2432657.832 | 0.014 | −1409 |
| 24b | 2432658.855 | 0.124 | −1104 |
| 24b | 2432659.877 | 0.234 | 1155 |
| 24b | 2432660.900 | 0.344 | 1900 |
| 24b | 2432661.829 | 0.444 | 2335 |
| 24b | 2432693.804 | 0.883 | −1045 |
| 24b | 2433041.809 | 0.321 | 1754 |
| 24b | 2433042.831 | 0.431 | 1723 |
| 24b | 2433046.828 | 0.861 | −28 |
| 24b | 2433047.758 | 0.961 | −1776 |
| 24b | 2433048.780 | 0.071 | −1944 |
| 24b | 2433075.735 | 0.971 | −1826 |
| 24b | 2433077.780 | 0.191 | 928 |
| 24b | 2433313.037 | 0.500 | 2515 |
| 24b | 2433316.011 | 0.820 | −244 |
| 24b | 2433330.976 | 0.430 | 1937 |
| 24b | 2433331.999 | 0.540 | 1980 |

**Note.** (1) Set No. is from Table 7, (2) Phase is calculated from the ephemeris JD = 2440382.250 + 9.29548$E$.

magnetic field of CS Vir, Babcock published the epoch ($E_{\rm calc} = ({\rm JD} - {\rm JD}_0)/P_0$) for each spectrogram he analyzed according to his ephemeris of JD = 2430143.070 + 9.295$E$, so we were able to determine the JD for each spectrogram. He also published magnetic field measurements for several lines on each spectrogram; we averaged his values for lines of Fe I, Fe II and Ti II. These values represent DS24b; they are given in Table 8. The scatter in these values is large, but less than that of DS23b.

A period change of 660 ms yr$^{-1}$ predicts a phase change of 0.06 between DS17b and DS23b and 0.04 between DS24b and DS34b. We cannot directly compare the $v$ photometry with the line intensity data (Figure 7) although they appear to be mirror images of each other with extrema at a phase of 0.5 and the phase differences from their respective curve fits is only 0.02. However, we cannot rule out a larger phase shift, due to the large scatter in DS23b. Although there are eleven magnetic field data sets for CS Vir, only DS 24b and DS34b are separated by a large

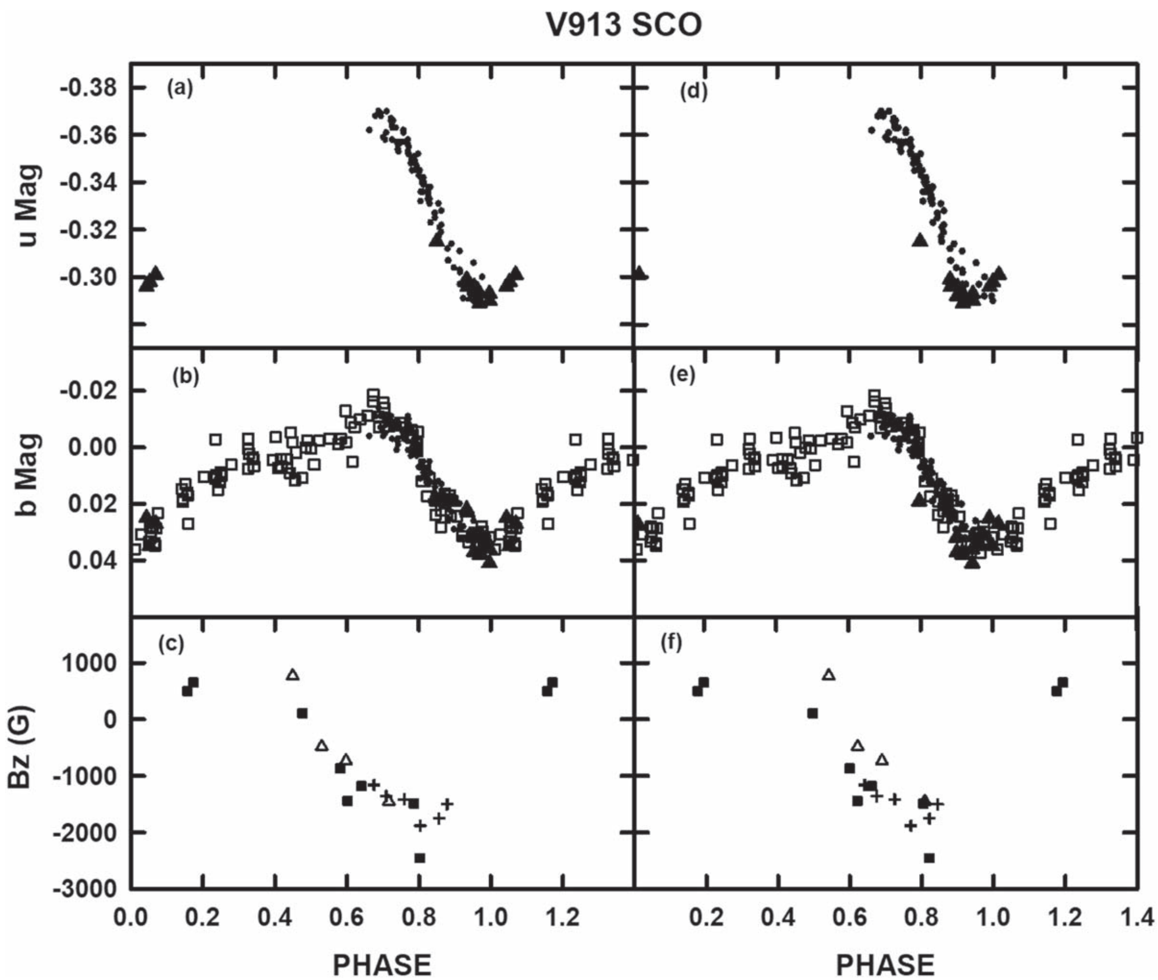


**Figure 8.** Photometric and magnetic variations of V913 Sco. Closed triangles, open squares and closed circles are the values of DS1c, 6c and 7c, respectively. Closed squares, pluses and open triangles are the *Bz* values of DS2c, 3c and 5c, respectively. Phases for (a)–(c) are calculated from the ephemeris JD = 2448267.593 + 0.979077 *E*; phases for (d)–(f) are from Model 2 (see text).

enough time interval to show an appreciable predicted phase shift. These two magnetic data sets are compared directly in Figure 7, but again we cannot say definitively that there is no shift because of the scatter in the DS24b data. It should be noted that the period of 9.29548 days derived from the FCAPT data is the same within the errors of measurement as the period of 9.29545 days derived by Leone & Catanzaro (2001) and the period of 9.29558 days derived by Rusomarov et al. (2016). Likewise, the predicted phase difference between the 2011 *STEREO* data (DS22b) and the Stibbs data (DS1b) is also 0.04 and the measured phase difference between the maxima of the two data sets is only 0.005 but we do not have the light curve data for DS22b for a direct comparison.

In summary, there is no evidence for a period change in CS Vir when the FCAPT data are included.

### 4.3. V913 Sco = HD 142990

We obtained FCAPT *uvby* data for this star from 1992–2005 (Table 1, Table A3). The previously published observations of this star are discussed below. Table 9 summarizes the photometric and magnetic data available for V913 Sco. We began with the assumption that the period of V913 Sco is that of Catalano & Leone (1996), $P = 0.97907 \pm 0.00001$ day (DS7c). This period also fits the *Hipparcos* (ESA 1997) data (DS6c). The only photometry prior to 1990 is that of Pedersen & Thomsen (1977) (DS1c), which only covers a small portion of the variation cycle, but the *u* values are well-defined and appear to show a minimum in brightness. We assumed that this was the case and found that all three data sets match well when plotted with $P = 0.979077 \pm 0.000003$ day (see Figures 8(a), (b)). Bohlender et al. (1993) compared their magnetic *Bz* data

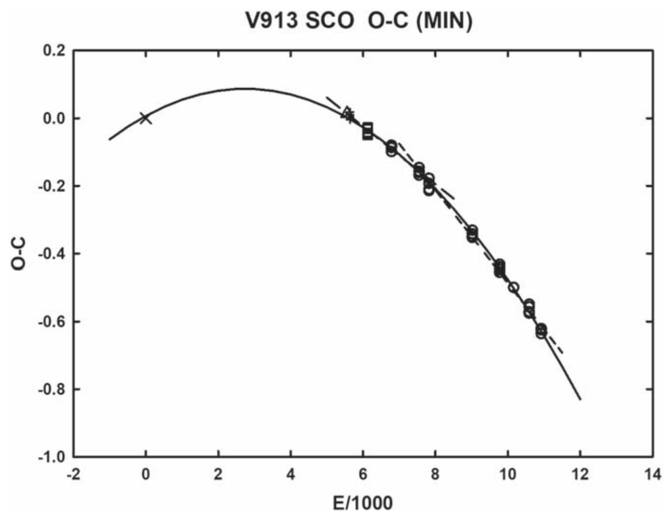


**Figure 9.** $O - C$ plot for V913 Sco. Except as noted in Table 9, *uvby* magnitudes are plotted for each data set. Open circles are the FCAPT data (DS9c-19c); DS1c, 6c, 7c and 8c are represented by crosses, open triangles, pluses and open squares, respectively. The solid curve is a 2nd order polynomial fit to all the data; the long-dashed line is the linear fit for DS6c-11c ($P_2$) and the short-dashed line is a linear fit for DS12c-19c ($P_3$).

**Table 9**
Data Sets for V913 SCO

| Set No. | Yrs Obs | No. | Comments | Used? | References |
|---|---|---|---|---|---|
| 1c | 1976 | 12 | 1 | Y *u* | Pedersen & |
| | | | | N *vby* | Thomsen (1977) |
| 2c | 1978 | 8 | | N MF | Borra et al. (1983) |
| 3c | 1982 | 6 | | N MF | Borra et al. (1983) |
| 4c | 1981 | 6 | | N *vby* | Borra et al. (1985) |
| 5c | 1988 | 5 | | N MF | Bohlender et al. (1993) |
| 6c | 1990–93 | 111 | 2 | Y *Hp* | *Hipparcos* (ESA 1997) |
| 7c | 1991 | 94 | | Y *uvby* | Catalano & Leone (1996) |
| 8c | 1991–94 | 54 | | Y *uvby* | Manfroid et al. (1991) |
| 9c | 1992–93 | 21 | | N *uvby* | FCAPT this paper |
| 10c | 1993–94 | 52 | | Y *uvby* | FCAPT this paper |
| 11c | 1994–95 | 9 | | N *uvby* | FCAPT this paper |
| 12c | 1995–96 | 48 | | Y *uvby* | FCAPT this paper |
| 13c | 1996–97 | 39 | | Y *uvby* | FCAPT this paper |
| 14c | 1999–2000 | 18 | | Y *uvby* | FCAPT this paper |
| 15c | 2000–01 | 12 | | N *uvby* | FCAPT this paper |
| 16c | 2001–02 | 26 | | Y *uvby* | FCAPT this paper |
| 17c | 2002–03 | 49 | 1 | Y *u* | FCAPT this paper |
| | | | | N *vby* | |
| 18c | 2003–04 | 69 | | Y *uvby* | FCAPT this paper |
| 19c | 2004–05 | 24 | | Y *uvby* | FCAPT this paper |

**Note.** (1) No. = Number of data points, (2) Y = Yes, (3) N = No, (4) MF = magnetic field, (5) Comments: 1: Large scatter *vby*; 2: Only single filter.

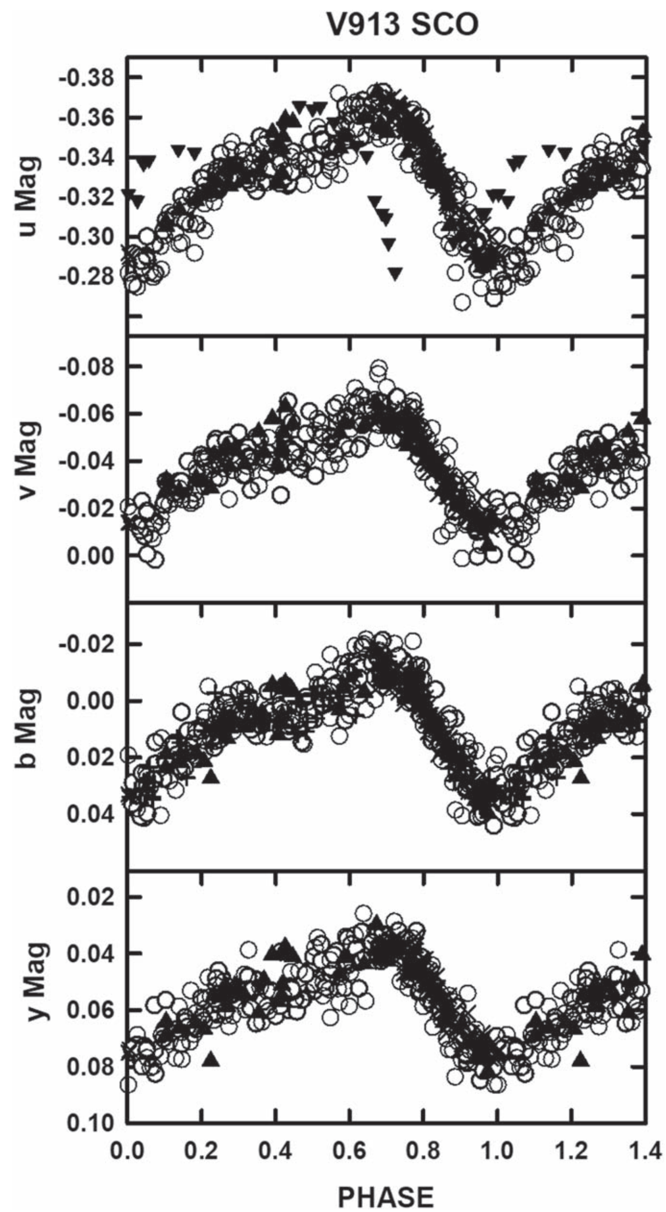


**Figure 10.** Photometric variations for V913 Sco. The FCAPT data are open circles (DS10c-19c); pluses, crosses, and closed triangles are DS6c, 7c, 8c and, respectively. Phases are for $P_2$ (see text). In the *u* plot, the closed triangles are the uncorrected DS19c data points, to show the shift due to the period change.

(DS5c) with those of Borra et al. (1985) (DS2c, DS3c) and found several possible periods; one of these was $P = 0.97909 \pm 0.00001$ day. These three data sets also match when plotted with the 0.979077 day period (Figure 8(c)). When we plotted the Long-Term Photometric Variable (LTPV) data (DS8c) (Manfroid et al. 1991) and the FCAPT data (DS9c-19c)

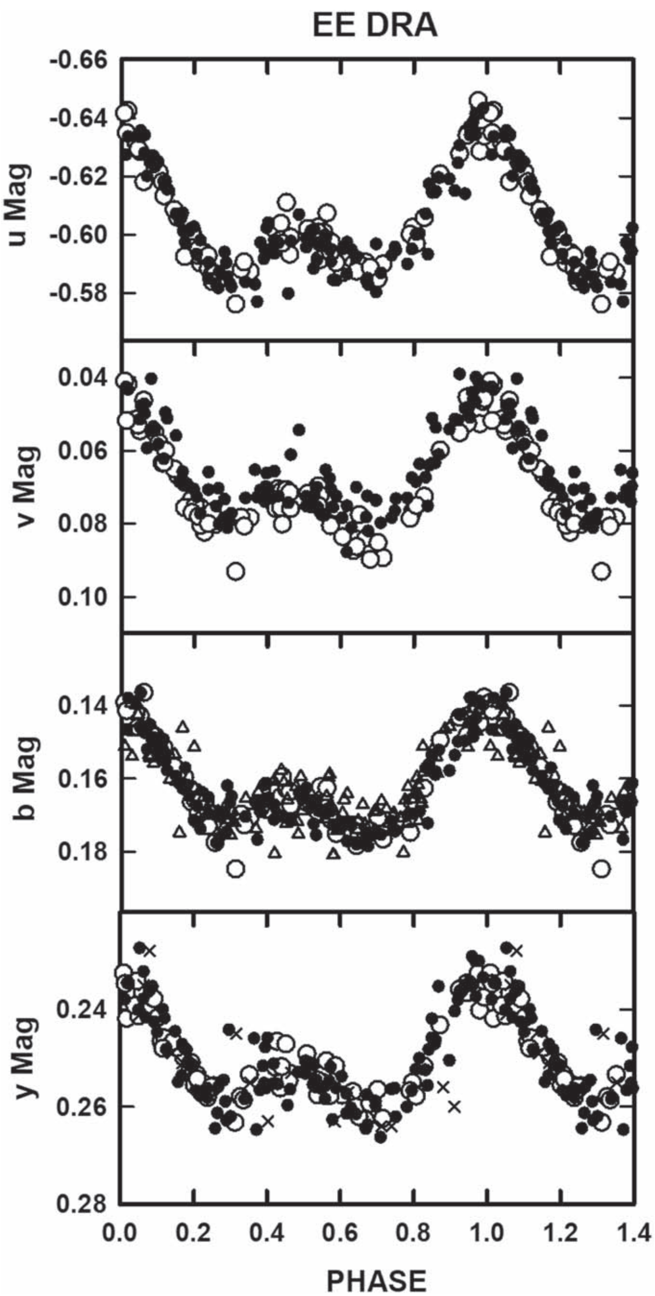


**Figure 11.** Photometric data for EE Dra. Open circles represent FCAPT 1994–95, closed circles represent FCAPT 2010–11, open triangles represent *Hipparcos Hp* and crosses represent Winzer *V*. Phases are calculated from the ephemeris JD = 2455846.579 + 1.123250 *E*.

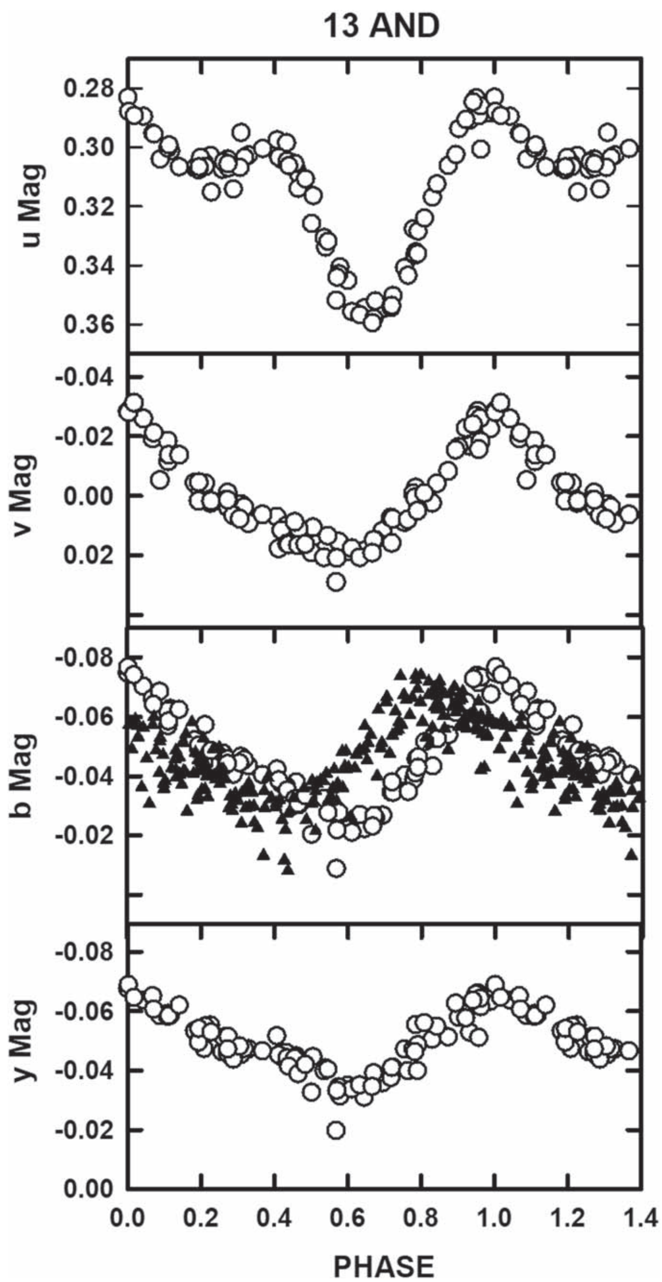


**Figure 12.** Photometric variations of 13 And. Open circles represent the FCAPT *uvby* values and closed triangles are the *Hipparcos Hp* values. Phases are calculated from the ephemeris JD = 2453276.832 + 1.47926 *E*.

with the same period, however, we found phase shifts indicating that the period was decreasing.

We then did an $O - C$ analysis based on the data sets in Table 9. The data sets indicated in the table as not included were DS4c, 9c, 11c, and 15c, due to incomplete phase coverage and small number of data points. The Catalano & Leone data (DS7c) also only covers a phase range of about 0.3, but within that range, the shapes of the light curves are well-determined; we found the phase of light minimum from comparison with the curve fit for DS12c. Although the LTPV (DS8c) data were obtained from 1991–94, each year has incomplete phase coverage, so we combined all the data to determine the light minima. We chose $JD_0$ = 2442826.849, the Pedersen & Thomsen (DS1c) minimum, and $P_0 = 0.979077$ see (Equation (1)); the plot is shown in Figure 9. As for V901 Ori, the plot can be interpreted as either a

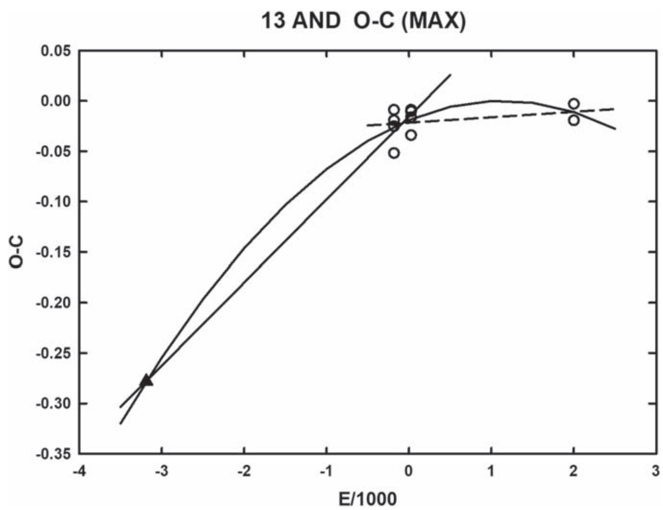


**Figure 13.** $O - C$ plot for 13 And. The symbols are the same as in Figure 12. The solid curve is a 2nd order polynomial fit to all the data; the solid line is the linear fit for DS1d-4d and the dashed line is a linear fit for DS3d-5d.

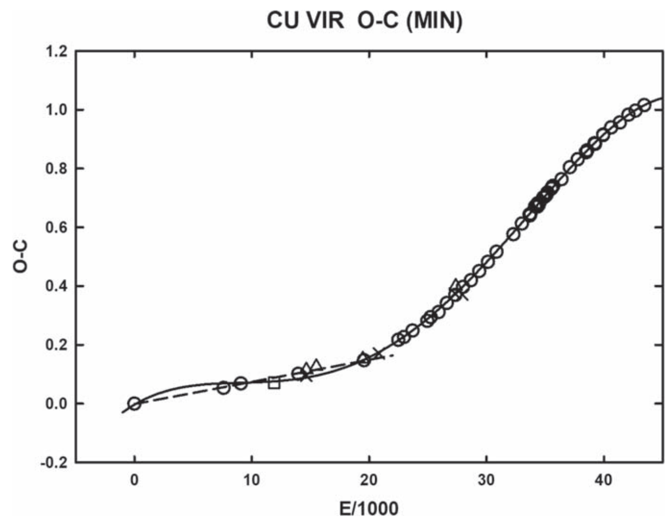


**Figure 14.** $O - C$ plot for CU Vir. Open circles represent the photometry data discussed in the text; the open square is the Winzer (1974) data. Open triangles and crosses are the He I and Si II data in Table 11, respectively. The solid curve is the 4th order polynomial fit to all the photometry, and the dashed line is the linear fit to the photometric data prior to 1985.

sequence of discrete period changes, Model 1 (M1), or a linear period change, Model 2 (M2).

If we assume M1, we need three periods: $P_1 = 0.979077$ (before 1988), $P_2 = 0.978992$ (1991–96), and $P_3 = 0.978940$ (1996–2004); the $P_2$ to $P_3$ change occurs in 1996. Figure 10 shows *uvby* normalized plots of all the photometry except DS1c, plotted with the ephemeris for $P_2$, JD $= 2450216.765 + 0.978992E$; DS13c-19c have phase shifts added to account for the difference between $P_2$ and $P_3$.

If the period linearly changes (M2), the 2nd order polynomial fit results in a period decrease of 690 ms yr$^{-1}$ ($\alpha = -2.14 \times 10^{-8}$ seconds per cycle). This is the largest period change found so far for an mCP star (see Mikulášek 2016). To see how M1 compares with M2, we calculated $P_{cc}$ using Equation (3), as we did for V901 Ori, with $P_m = 0.979087$ and $E_m = 446.3$. We used the *u* and *b* photometry and magnetic field data for DS1c-3c, DS6c and DS7c, and added the appropriate phase shifts to convert to $P_1$; the results are plotted in Figure 8. As is shown in Figure 8, the M2 plots (Figures 8(d)–(f)) data fits are not quite as good as for M1 (Figures 8(a)–(c)), but as was the case for V901 Ori, we cannot clearly distinguish between the models.

### *4.4. EE Dra = HD 177410*

Adelman (2004) reported on the extraordinary photometric behavior of EE Dra (HR 7224) during the FCAPT observing periods of 2002–03 and 2003–04. Adelman was concerned about these bizarre results, so he obtained FCAPT observations for this star every year from the observing periods 2004–2005 through 2012–2013 (Tables 1, Table A4). We found that the best fit to the *Hipparcos* (ESA 1997) *Hp* and the FCAPT *uvby* light curves for the time intervals 1993–95 and for 2004–13 was with a period of $1.123250 \pm 0.000004$ days. This is shown in Figure 11, where we plot the FCAPT data for the observing periods of 1994–95 and 2010–11, as well as the *Hipparcos* and Winzer *UBV* data (1974). The period is well-established due to the large amount of FCAPT data from 2004–2013.

The problem remains to explain the aberrant results for the FCAPT data from 2001–04. We found some clues when we assessed all our data after the FCAPT ceased operation in 2013. We compiled a list for all our program stars, noting which years we discarded the data and the reasons for this. We noticed that in 2001–02, 18 out of 34 stars were discarded and in 2002–03, 16 out of 19 stars were discarded. For three stars, much of the data had to be discarded but some were OK; those three stars all have southern declinations. In addition, most of the data in the first half of 2003–04 had to be discarded for all the 22 stars observed that year. Mostly, the reason for discarding these data was excessive scatter. We suspect that an imbalance of the telescope that occurred during 2002–03, the first half of 2003–04 and possibly also in 2001–02, was responsible for these results. The discrepant behavior of EE Dra during this time interval was the most extreme but it should be noted that EE Dra has the highest northern declination of the stars we observed with the FCAPT during this time interval. For an Alt-Azimuth telescope such as the

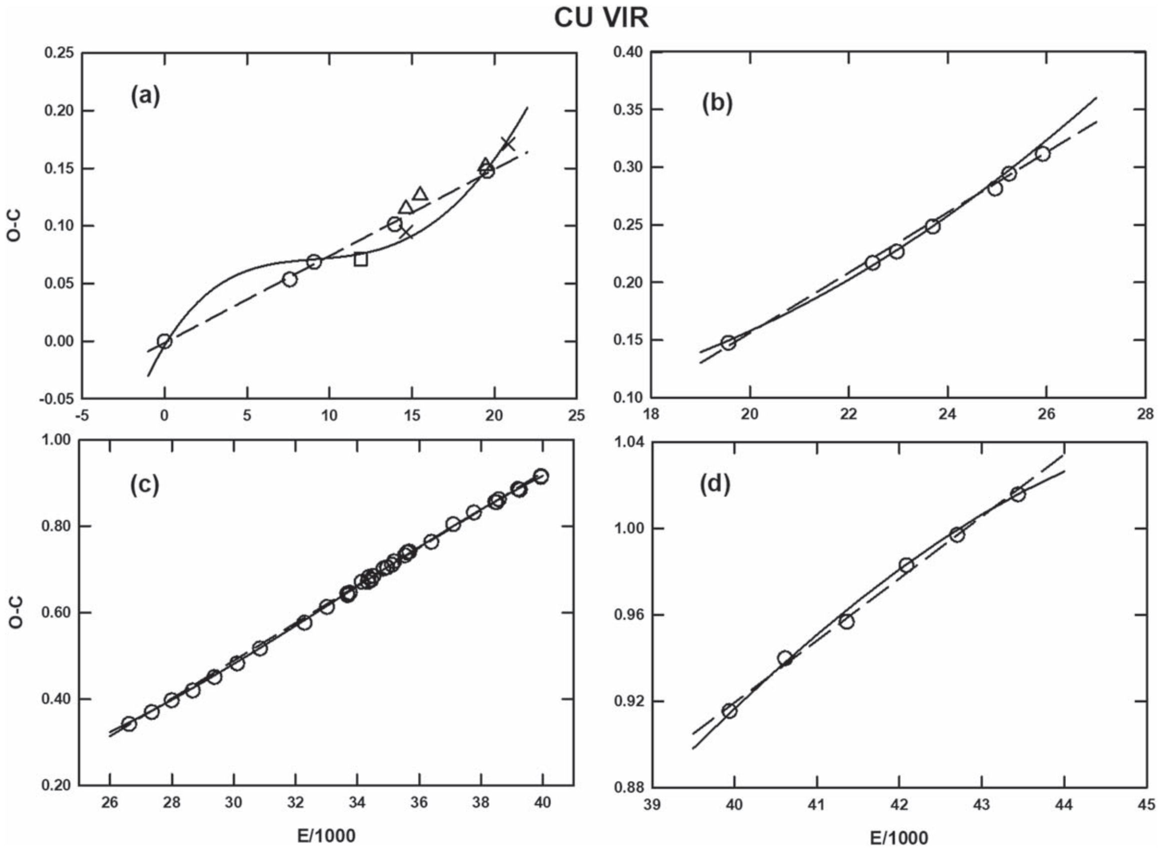


**Figure 15.** $O - C$ plots for CU Vir. Comparison of linear (dashed line) with 4th order polynomial (solid line) regressions. The symbols are the same as in Figure 14. Time intervals are: (a) 1958–83; (b) 1979–92; (c) 1993–2011; (d) 2012–17. Linear regressions represent $P_1$, $P_2$, $P_3$ and $P_4$ for (a), (b), (c), and (d), respectively. Note the different scales.

**Table 10**
Data Sets for 13 AND

| Set No. | Yrs Obs | No. | Comments | Used? | References |
|---|---|---|---|---|---|
| 1d | 1990–93 | 195 | 1 | Y *Hp* | *Hipparcos* (ESA 1997) |
| 2d | 2000–01 | 5 | | N *uvby* | FCAPT Adelman (2005) |
| 3d | 2003–04 | 23 | | Y *uvby* | FCAPT Adelman (2005) |
| 4d | 2004–05 | 38 | | Y *uvby* | FCAPT Adelman (2005) |
| 5d | 2012–13 | 23 | | Y *uvby* | FCAPT this paper |

**Note.** (1) No. = Number of data points, (2) Y = Yes, (3) N = No, (4) Comments: 1: Only single filter.

FCAPT, the pointing algorithm is less stable for stars with more northernly declinations.

### 4.5. 13 And = HD 220885

Adelman (2005) compared his 2003–2005 observations with the *Hipparcos* photometry and found a period of 1.47931 days for 13 And. There are no spectrum or magnetic variations published for this star.

Since his 2005 paper Adelman obtained one more set of FCAPT *uvby* data in 2012–13 for 13 And (Table 1, Table A5). We were surprised to find that this data set showed a phase shift when compared with the previous data, indicating a shorter period. All the data sets are summarized in Table 10 and the light curves are shown in Figure 12.

To clarify the situation, we carried out an $O - C$ analysis (Figure 13); DS2d was not used due to the small number of data points and incomplete phase coverage. We chose

**Table 11**
Data Sets for CU VIR

| Set No. | Yrs Obs | No. | Type | References |
|---|---|---|---|---|
| 1e | 1967–76 | 20 | $W_\lambda$: Si II, He I | Hardorp & Megessier (1977) |
| 2e | 1977 | 69 | $W_\lambda$: He I | Pedersen (1978) |
| 3e | 1983 | 9 | $W_\lambda$: He I | Hiesberger et al. (1995) |
| 4e | 1985–87 | 14 | $W_\lambda$: Si II | Hatzes (1997) |
| 5e | 1994–95 | 19 | $W_\lambda$: He I | Kuschnig et al. (1999) |
| 6e | 1993–95 | 40 | $W_\lambda$: Si II | Pyper et al. (1998) |
| 7e | 1997–98 | 190 | *uvby* | Pyper et al. (2013) |
| 8e | 1998–99 | 113 | *uvby* | Pyper et al. (2013) |
| 9e | 2000–01 | 102 | *uvby* | Pyper et al. (2013) |
| 10e | 2001–02 | 70 | *uvby* | Pyper et al. (2013) |
| 11e | 2002–03 | 122 | *uvby* | Pyper et al. (2013) |
| 12e | 2003–04 | 54 | *uvby* | Pyper et al. (2013) |
| 13e | 2004–05 | 86 | *uvby* | Pyper et al. (2013) |
| 14e | 2005–06 | 100 | *uvby* | Pyper et al. (2013) |
| 15e | 2006–07 | 89 | *uvby* | Pyper et al. (2013) |
| 16e | 2007–08 | 102 | *uvby* | Pyper et al. (2013) |
| 17e | 2008–09 | 199 | *uvby* | Pyper et al. (2013) |
| 18e | 2009–10 | 168 | *uvby* | Pyper et al. (2013) |
| 19e | 2010–11 | 127 | *uvby* | Pyper et al. (2013) |
| 20e | 2011–12 | 354 | *uvby* | Pyper et al. (2013) |
| 21e | 2012 | 401 | *BV* | Krtiĉka et al. (2019) |
| 22e | 2013 | 68 | *BV* | Krtiĉka et al. (2019) |
| 23e | 2014 | 84 | *BV* | Krtiĉka et al. (2019) |
| 24e | 2015 | 59 | *BV* | Krtiĉka et al. (2019) |
| 25e | 2016 | 184 | *BV* | Krtiĉka et al. (2019) |
| 26e | 2017 | 263 | *BV* | Krtiĉka et al. (2019) |

**Note.** (1) No. = Number of data points, (2) $W_\lambda$ = Equivalent width.

$JD_0 = 2453276.832$, the DS4d maximum, and $P_0 = 1.47926$ (see Equation (1)). The results of the analysis are that DS1d, 3d and 4d are consistent with a constant period of 1.47934 days and DS3d, 4d and 5d fit a period of 1.47926 days (Figure 12).

With so few data sets, a continuous period change cannot be ruled out, and if we fit a 2nd order polynomial to the $O-C$ data, we find a linear period decrease of $\alpha = -2.98 \times 10^{-8}$ days per cycle or a decrease of 640 ms $yr^{-1}$.

## 5. Further Analysis of CU Vir (HD 124224)

Krtiĉka et al. (2019) have published a new study of CU Vir which includes photometric *BV* magnitudes obtained by G. Henry from 2012–17. This photometry indicates a decrease in the period compared to the period for the time interval 1993–2011, as determined by Pyper et al. (2013). Krtiĉka et al. assume that the period change is continuous for this star and show an $O-C$ plot demonstrating the period change. We were interested to see whether we could distinguish a model with discrete period changes from one with continuous changes, so we added the most recent photometric data to the photometric data tabulated in Pyper et al. (1998) plus the Henry, Liška, and Janik and Liška *UBV* data tabulated in Mikulášek et al. (2011), and calculated a new $O-C$ plot (Figure 14) based on the same $JD_0 = 2435256.755$ and $P_0 = 0.52037$ used in the 2013 paper. The data points represent averages of light minima over all the filters measured in each data set. Table 11 summarizes the FCAPT data sets after 1997, included but not tabulated in the 2013 paper, and the recent *BV* data, which were not tabulated in the 2019 paper, as well as the most complete He I and Si II data sets. The latter were not used in our $O-C$ analysis but are plotted for comparison. The Winzer (1974) *UBV* data were not included in the analysis due to the small number of data points and because the minimum was not observed. These data were also plotted for comparison. Figure 14 includes all the data used in the 2013 paper, including the Solar Mass Ejection Imager data, as well as the more recent data in Table 11.

The results for the discrete period change model are: $P_1 = 0.5206775$ (1958–83), $P_2 = 0.5206961$ (1979–92), $P_3 = 0.5207140$ (1993–2011), and $P_4 = 0.5206987$ (2012–17). The first three periods are the same as those in the 2013 paper within the errors of measurement; $P_4$ is determined from a linear fit to the $O-C$ values of DS21e-26e.

Figure 15 illustrates the linear regression fits of the data compared to the 4th order polynomial fit for four different time intervals. As can be seen, the fits are equally good for $P_2$, $P_3$ and $P_4$; the linear fit for $P_1$ is slightly better than the polynomial fit. Thus, as is the case for V901 Ori, V913 Sco and 13 And, we cannot distinguish between discrete period change and continuous change models for CU Vir.

## 6. Discussion and Conclusions

As we mentioned in Section 3, we have obtained *uvby* FCAPT photometry for 87 mCP stars. Of these, 75 stars have large enough amplitudes of variation in *uvby* to check for period changes. In all, there are five stars, 56 Ari, V901 Ori, V913 Sco, 13 And and CU Vir, that show changes in their periods. With so few stars, it is difficult to generalize, but all five have short rotational periods ranging from 0.5 day (CU Vir) to 1.5 days (V901 Ori, 13 And). Their temperatures range from 13,000 K for CU Vir to 23,000 K for V901 Ori. As regards the period changes we found, V901 Ori shows a period increase, while V913 Sco and 13 And show decreasing periods; previous investigations show that the period increases then decreases for CU Vir. Adelman et al. (2001) also found that 56 Ari shows a small period increase. Two other stars not observed with the FCAPT, $\sigma$ Ori E and BS Cir, are reported by Mikulášek (2016) to have increasing periods. Mikulášek suggests that $\sigma$ Ori E, an eclipsing binary, may have a stellar wind strong enough to cause the increase in the period. In the case of BS Cir, he suggests that precession may be the cause of the changes he observed from photometric data obtained after 2000.

The question arises as to why only five of the stars we checked display period changes. The answer is that the periods of many of the stars may change, but the existing data are not adequate to detect the changes. The phase shift, $\Delta\phi$, resulting from a period change is given by

$$\triangle\varphi = 0.5 \times \triangle T \times \left(\frac{1}{P} - \frac{1}{P + \triangle P}\right), \qquad (4)$$

where $\Delta T$ is the time interval over which the data were collected and $\Delta P$ is the change in the period over this time interval. If we assume a star's period is changing linearly, $\Delta P = \alpha \Delta T$, where $\alpha$ is the rate of change. For most of the FCAPT light curves and many of the previously published data we can detect phase shifts of $\geqslant 0.04$, so we can estimate the minimum period change, $\Delta P_{\min}$, that can be detected for these 75 stars; $\Delta T$ ranges from 6 to 62 yr, including previously published data. The small period changes of 56 Ari and CU Vir were detected due to their short periods and the longer time intervals over which they were observed. Only two other stars have $\Delta P_{\min} < 20\,\mathrm{ms\,yr^{-1}}$ and can be assumed to have constant periods; most of the other stars could also have period changes that have not been detected. For 40 stars, the values of $\Delta P_{\min}$ are small enough that we can ascertain that the larger period changes detected in V901 Ori, V913 Sco and 13 And do not occur. Currently, then, there is a large amount of uncertainty as to how many mCP stars have changing periods; higher precision photometry and/or longer time intervals of observation will be required to detect possible period changes. For example, MN Ser has the longest period of the 75 stars in our sample; it has $P = 18.1$ days, $\Delta T = 40$ yr and $\Delta P_{\min} = 4060\,\mathrm{ms\,yr^{-1}}$. It would require $\Delta T = 100$ yr to reduce $\Delta P_{\min}$ to $620\,\mathrm{ms\,yr^{-1}}$ and 400 yr for $\Delta P_{\min} = 40\,\mathrm{ms\,yr^{-1}}$.

For V901 Ori, CU Vir and V913 Sco, all data after the start of the FCAPT observations (1990) show equally good agreement with linear (continual for CU Vir) or discrete period changes, but data prior to 1990 show slightly better agreement with discrete period changes. All we can say about 13 And is that the period decreased at some time after 1994.

The discovery of two stars with decreasing periods may strengthen the case for some sort of oscillation, if we assume the periods change continuously. Stępień (1998) first proposed that the cause might be torsional oscillations due to the interaction between the rotation of a star and its magnetic field. Krtĉka et al. (2017) made torsional oscillation calculations for CU Vir and V901 Ori to compare with the observed period changes. They found a rough agreement between the calculated period of oscillation and their observed period for CU Vir, assuming its period changes continually; this result remains the same including the recent data showing a decrease in the period after 2012 (Krtĉka et al. 2019). However, for V901 Ori, they estimate the observed period of oscillation to be greater than 100 yr, but the torsional oscillation calculations predict a much shorter period. This disparity is probably even larger for V901 Ori, because the 2017 paper assumed that it shows a decrease in its period starting in 2003, based on the data available to them at the time, but the addition of the FCAPT data for this star shows no decrease in the period through 2012. The data for V913 Sco show a decreasing period over a time interval of 38 yr with no indication of a period increase, so the situation may be similar to that of V901 Ori. We cannot reach a conclusion about 13 And due to the small amount of data for this star. Thus, it is possible that torsional oscillations may cause the period changes only for CU Vir but not V901 Ori and probably not for V913 Sco and 13 And. This result suggests that either the small period change in CU Vir (and possibly 56 Ari) is a special case and the significantly larger variations in the other stars are due to some other type of oscillation (unknown at present) or that torsional oscillations are not the cause of any of the period changes. We re-emphasize that only CU Vir has been observed to change from a period increase to a decrease, so if they are oscillating, the other four stars have very long periods.

The discrete period change model for these stars is also difficult to explain. In order to explain the period increase reported by Pyper et al. (1998), Stępień (1998) suggested that the density distribution in the envelope of the star may abruptly change from a prolate to an oblate configuration due to the interaction between the meridional circulations with the magnetic field near the boundary between the envelope and the interior. It is not clear whether this explanation works for a discrete decrease in the period, however and no one so far has attempted to model this, so it remains speculative.

This work was supported in part by NSF grants AST-9115114, AST 9528506, AST-0071260, and NSF AST-0507381 to The Citadel and UNLV and in part by grants from The Citadel Foundation. This research has used the SIMBAD database, operated at the CDS, Strasbourg, France. We would like to thank our reviewer for carefully reading the paper and for many helpful suggestions.

## References

Adam, M. G. 1965, Obs, 85, 204
Adelman, S. J. 1997, A&AS, 125, 65
Adelman, S. J. 2004, MNRAS, 351, 823
Adelman, S. J. 2005, PASP, 117, 476
Adelman, S. J. 2006, PASP, 118, 77
Adelman, S. J., Malanushenko, V., Ryabchikova, T. A., & Savanov, I. 2001, A&A, 375, 982
Adelman, S. J., & Pyper, D. M. 1985, A&AS, 62, 279
Babcock, H. W. 1951, ApJ, 114, 1
Babcock, H. W. 1958, ApJS, 3, 141
Bartolini, C., Bonifazi, A., Fusi Pecci, F., et al. 1982, Ap&SS, 83, 287
Blanco, C., Catalano, F. A., & Strazzulla, G. 1978, A&AS, 31, 205
Bohlender, D. A., Landstreet, J. D., & Thompson, I. B. 1993, A&A, 269, 355
Borra, E., Beaulieu, A., Brousseau, D., & Shelton, I. 1985, A&A, 149, 266
Borra, E. F., & Landstreet, J. D. 1979, ApJ, 228, 809
Borra, E. F., & Landstreet, J. D. 1980, ApJS, 42, 421
Borra, E. F., Landstreet, J. D., & Thompson, I. 1983, ApJS, 53, 151
Catalano, F. A., Kroll, R., & Leone, F. 1992, A&A, 263, 203
Catalano, F. A., & Leone, F. 1996, A&A, 311, 230
Deutsch, A. J. 1947, ApJ, 105, 283
Donati, J.-F., Semel, M., Carter, B. D., et al. 1997, MNRAS, 291, 658
ESA 1997, The Hipparcos and Tycho Catalogs, SP-1200 (Noordwijk: ESA)
Hardorp, J., & Megessier, C. 1977, A&A, 61, 411
Hatzes, A. P. 1997, MNRAS, 288, 153

Hiesberger, F., Poskunov, N., Bonsack, W. K., et al. 1995, A&A, 296, 473
Hockey, M. S. 1971, MNRAS, 152, 97
Hoffleit, D. 1982, The Bright Star Catalogue (4th ed.; New Haven: Yale Univ. Observatory)
Hoffleit, D., Saladyga, M., & Wlasuk, P. 1983, A Supplement to the Bright Star Catalogue (New Haven: Yale Univ. Observatory)
Krtiĉka, J., Mikulášek, J., Henry, G. W., et al. 2017, MNRAS, 464, 933
Krtiĉka, J., Mikulášek, J., Henry, G. W., et al. 2019, A&A, 625, 34
Kuschnig, R., Ryabchikova, T. A., Riskuov, N. E., & Weiss, W. W. W. 1999, A&A, 348, 924
Landstreet, J. D., Borra, E. F., Angel, J. R. P., & Illing, R. M. E. 1975, ApJ, 201, 624
Leone, F., & Catanzaro, G. 2001, A&A, 365, 118
Maitzen, H. M., & Moffat, A. F. J. 1972, A&A, 16, 385
Maitzen, H. M., & Rakosch, K. D. 1970, A&A, 7, 10
Manfroid, J., Sterken, C., Bruch, A., et al. 1991, A&AS, 87, 481
Mathys, G. 1994, A&AS, 108, 547
Mathys, G., & Hubrig, S. 1997, A&AS, 124, 475
Mikulášek, Z. 2016, CoSka, 46, 95
Mikulášek, Z., Krtiĉka, J., Henry, G. W., et al. 2008, A&A, 485, 585
Mikulášek, Z., Krtiĉka, J., Henry, G. W., et al. 2011, A&A, 534, L5
Ozuyar, D., Sener, H. T., Stevens, I. R., et al. 2018, PASA, 35, 40
Pedersen, H. 1978, A&AS, 33, 203
Pedersen, H. 1979, A&AS, 35, 313
Pedersen, H., & Thomsen, B. 1977, A&AS, 30, 11
Pyper, D. M., & Adelman, S. J. 1985, A&AS, 59, 369
Pyper, D. M., Ryabchikova, T. A., Malanushenko, V., et al. 1998, A&A, 339, 822
Pyper, D. M., Stevens, I. R., & Adelman, S. J. 2013, MNRAS, 431, 2106
Rusomarov, N., Kockukhov, O., Ryabchikova, T. A., & Ilying, I. 2016, A&A, 588, A138
Shore, S. N., & Brown, D. N. 1990, ApJ, 365, 665
Stępień, K. 1998, A&A, 337, 754
Stibbs, D. W. N. 1950, MNRAS, 110, 395
Strassmeier, K. G., & Hall, D. D. S. 1988, ApJ, 67, 439
Thompson, I. B., & Landstreet, J. D. 1985, ApJ, 289, 9
Winzer, J. E. 1974, PhD thesis, Univ. of Toronto
Wolff, S. C., & Wolff, R. J. 1971, AJ, 76, 422